Downregulation of miR-29b-3p promotes α-tubulin deacetylation by targeting the interaction of matrix metalloproteinase-9 with integrin β1 in nasal polyps

ZHUOHUI LIU[1*], HAOYU LIU[2*], DESHUN YU[3], JINGYU GAO[1], BIAO RUAN[1] and RUIQING LONG[1]

[1]Department of Otolaryngology, The First Affiliated Hospital of Kunming Medical University, Kunming, Yunnan 650032;
[2]Department of Otolaryngology, The First People's Hospital of Qujing, Qujing, Yunnan 655000;
[3]Department of Otolaryngology, Affiliated Hospital of Dali University, Dali, Yunnan 671000, P.R. China

Received November 10, 2020; Accepted April 12, 2021

DOI: 10.3892/ijmm.2021.4959

Abstract. Matrix metalloproteinase (MMP)-9 is a key enzyme responsible for extracellular matrix degradation and contributes to the progressive histological changes observed in lower respiratory tract infections. Integrin β1 and α-tubulin are potential MMP-9-interacting proteins, and microRNA (miR)-29b-3p can regulate MMP-9 expression. MMP-9 is highly expressed in chronic rhinosinusitis with nasal polyps (CRSwNPs), regardless of its effects on miR-29b-3p, integrin β1 and α-tubulin expression. In the present study, samples from 100 patients with CRSwNPs were examined via reverse transcription-quantitative PCR to assess the mRNA expression of miR-29b-3p, and western blotting was performed to assess the protein expression of MMP-2, MMP-9, acetyl-α-tubulin, integrin β1 and tissue inhibitor of metalloproteinase 1 (TIMP-1). A dual-luciferase reporter assay was used to verify the direct binding of miR-29b-3p and MMP-2/MMP-9. Co-immunoprecipitation (Co-IP) and GST pull-down assays showed that integrin β1 and α-tubulin were MMP-9-interacting proteins. Cell viability, apoptosis and inflammatory cytokine levels were determined via a Cell Counting Kit-8 assay, flow cytometry and ELISA, respectively. miR-29b-3p expression was found to be positively correlated with MMP-2 and MMP-9 expression. Whereas, TIMP-1 expression was negatively correlated with MMP-2 and MMP-9 expression. The dual-luciferase assay revealed that miR-29b-3p targeted the 3' untranslated region of MMP-2/MMP-9. The Co-IP and GST pull-down assays showed that MMP-9 could directly bind to integrin β1 and indirectly bind to α-tubulin. Finally, the overexpression of miR-29b-3p decreased the expression of MMP-9 and increased the levels of acetyl-α-tubulin. By contrast, the knockdown of miR-29b-3p increased the expression of MMP-9 and decreased the levels of acetyl-α-tubulin. Additionally, MMP-9 expression was found to be negatively correlated with acetyl-α-tubulin expression. Of note, the expression of integrin β1 did not change following the overexpression and knockdown of MMP-9. Finally, the overexpression of miR-29b-3p not only decreased MMP-9 expression, but also alleviated lipopolysaccharide-induced inflammation in NP69 cells. The results showed that the downregulation of miR-29b-3p promoted α-tubulin deacetylation by increasing the number of MMP-9-integrin β1 complexes in CRSwNPs, thus targeting miR-29b-3p/MMP-9 may be a potential novel strategy for the clinical treatment of CRSwNPs.

Correspondence to: Dr Biao Ruan or Dr Ruiqing Long, Department of Otolaryngology, The First Affiliated Hospital of Kunming Medical University, 295 Xichang Road, Kunming, Yunnan 650032, P.R. China
E-mail: ruanbiaoent@163.com
E-mail: longrqent@163.com

*Contributed equally

Key words: chronic rhinosinusitis with nasal polyps, microRNA-29b-3p, matrix metalloproteinase-9, integrin β1, α-tubulin deacetylation

Introduction

Matrix metalloproteinases (MMPs) are zinc-dependent endopeptidases that have proteolytic activity and play vital roles in a number of physiopathological processes, such as experimental autoimmune encephalomyelitis and breast cancer (1-3). Tissue remodeling processes involve the thinning of the basement membrane, glandular changes and accumulation of the extracellular matrix (4). MMPs can degrade specific extracellular matrix (ECM) components, suggesting that MMPs play a vital role in tissue remodeling (5,6). Alterations to the ECM can induce a range of cell behaviors, such as cell proliferation, migration and apoptosis (7,8). In addition, MMPs are regulated by a variety of biological processes, including transcription and posttranscription processes, and their main regulators are tissue inhibitors of matrix metalloproteinases (TIMPs) (9). Numerous studies have found that MMPs and TIMPs are specifically expressed in chronic rhinosinusitis with nasal polyps (CRSwNPs); for example, the levels of MMP-2 and MMP-9 are significantly increased in CRSwNPs, and the levels of TIMP-1 and TIMP-4 are significantly

decreased (10-13). In addition, corticosteroids and budesonide contribute to ameliorating inflammation by downregulating the expression of MMP-2 and MMP-9 (14) and upregulating the levels of TIMP-1, TIMP-2 and TIMP-4 (15). Thus, the balance between MMPs and TIMPs is important in tissue homeostasis within CRSwNPs (5).

Tubulin and microtubules (MTs) are the largest cytoskeletal components (16), and posttranslational modifications of tubulin are found in all cells with MTs (17,18). For example, acetyl-α-tubulin regulates MT stabilization and cell morphology (19,20). In addition, the loss of acetyl-α-tubulin is associated with TGF-β-induced epithelial-mesenchymal transition and sulfur mustard-induced chronic airway remodeling (21,22). A recent study showed that MMP-9 and integrins both act as regulators of α-tubulin acetylation and detyrosination (23), and Smith (24) found that MMP-9 can directly bind integrins to activate signaling pathways that involve cell adhesion molecules and pro-forms of growth factors (24). These studies suggested that MMP-9 binds to integrin proteins to regulate α-tubulin acetylation and deacetylation, and is involved in regulating polyp formation. Of note, a recent study showed that integrin β1 and α-tubulin proteins were potential MMP-9-interacting proteins (25). Thus, the present study aimed to pursue these ideas further.

It has been reported that microRNAs (miRNAs/miRs) can regulate the synthesis and degradation of ECM via the regulation of MMPs and TIMPs (26,27). For example, miR-29b-3p can directly and indirectly regulate MMP-2 and MMP-9 expression (28,29). A recent study showed that ciliogenesis and cilia function are significantly impaired in the CRSwNPs epithelium, presumably due to the altered expression of miRNAs (30). Zhang *et al* (31) found that overexpression of miR-30a-5p can attenuate the epithelial-mesenchymal transition by repressing CDK6 expression in nasal polyps (31). However, the relationships between miR-29b-3p and MMP-2/MMP-9 in regulating the progression of CRSwNPs are unclear.

Lee *et al* (23) found that MMP-9 and integrin β1 activity can increase α-tubulin acetylation. Of note, Smith (24) and Yin *et al* (25) found that integrin β1 is a potential MMP-9-interacting protein. Thus, we hypothesized that downregulation of miR-29b-3p promotes α-tubulin acetylation by increasing MMP-9 binding to integrin β1, and the present study aimed to provide novel insight into the etiology and pathogenesis of CRSwNPs.

Materials and methods

Patient tissue samples. The study group consisted of 100 patients (35 female and 65 male, median age of 42.7 years, age range of 18.2-83.6) who underwent functional endoscopic sinus surgery or septoplasty by a single surgeon at the Department of Otolaryngology, The First People's Hospital of Qujing (Qujing, China) between July 2018 and June 2019. Patients younger than 18 years old, with unilateral nasal polyps or with associated diseases, such as cystic fibrosis, inverted papilloma and ciliary dyskinesia were excluded from the present study. Each tissue was divided into four parts: One part was reserved for cell culture, one part was fixed for immunofluorescence evaluation using formalin for paraffin sectioning section or frozen sectioning, and the last two parts were stored at -80˚C for protein and mRNA extraction. The study was approved by the medical ethics committee of The First People's Hospital of Qujing, and written informed consent was obtained from each patient before participation in the study.

Isolation of primary human nasal epithelial cells (PHNECs) and cell lines. A human nasal epithelial cell line (NP69; cat. no. BNCC338439) and *Escherichia coli* BL21 competent cells (BL21; cat. no. BNCC353591) was purchased from BeNa Culture Collection; Beijing Beina Chuanglian Biotechnology Research Institute, human embryonic kidney 293T cells were purchased from The Cell Bank of Type Culture Collection of The Chinese Academy of Sciences. The MMP-2 and MMP-9 protein expression of 100 CRSwNPs tissues was determined via western blotting, and the CRSwNPs tissues with the lowest (Fig. S1; green box) and highest (Fig. S1; red box) expression of MMP-2 and MMP-9 were used to isolate PHNECs with the lowest and highest expression of MMP-2 and MMP-9 (L-PHNECs and H-PHNECs, respectively) as previously described (32). In brief, CRSwNPs tissue samples of ~1 ml volume were rinsed with normal saline, transferred into 10 ml DMEM/F12 medium (Thermo Fisher Scientific, Inc.) containing 1% penicillin/streptomycin (Sangon Biotech Co., Ltd.), digested with 0.1% protease from Streptomyces griseus (Thermo Fisher Scientific, Inc.) and 0.1 mg/ml deoxyribonuclease I (Sangon Biotech Co., Ltd.), and incubated at 4˚C overnight. Epithelial cells were removed by gentle scraping and dispersed into a single cell suspension. The medium was then transferred into a 15-ml conical tube and centrifuged at 300 x g for 5 min at room temperature. The supernatant was decanted, and the pellet was resuspended in DMEM/F12 medium.

RNA extraction and reverse transcription-quantitative (RT-q) PCR. Total RNA was extracted from CRSwNPs tissues or cells using TRIzol reagent (Invitrogen; Thermo Fisher Scientific, Inc.) according to the manufacturer's protocol. First-strand cDNA was synthesized from the total RNA according to the instructions of the PrimeScript™ RT Reagent Kit (Takara Biotechnology Co., Ltd.), and RT-qPCR was subsequently performed using the SYBR-Green qPCR kit (Thermo Fisher Scientific, Inc.), according to the manufacturer's protocols. The following primer sequences were used for RT-qPCR: miR-29b-3p forward, 5'-ACACTCCAGCTGGGTAGCACC ATTTGAAATC-3' and reverse, 5'-TGGTGTCGTGGAGTC G-3'; and U6 forward, 5'-CTCGCTTCGGCAGCACATA-3' and reverse, 5'-AACGATTCACGAATTTGCGT-3'. The RT-qPCR experiments were performed on an Applied Biosystems 7900HT Fast Real-time PCR system (Applied Biosystems; Thermo Fisher Scientific, Inc.). The following thermocycling conditions were used for RT-qPCR: Initial denaturation at 95˚C for 7 min; followed by 40 cycles of denaturation at 95˚C for 10 sec, annealing at 60˚C for 20 sec and elongation at 72˚C for 20 sec; and a final extension at 72˚C for 10 min. The relative expression levels were calculated using the $2^{-\Delta\Delta Cq}$ method (33) and normalized to those of internal reference gene U6.

Western blot assay. Proteins were extracted from CRSwNPs tissues or cells using radioimmunoprecipitation assay (Beyotime Institute of Biotechnology), and the concentrations

were determined according to the standard protocols of BCA protein assay kit (Beyotime Institute of Biotechnology), respectively. The total protein (30 μg/well) in the supernatant was separated via SDS-PAGE on 10% gel, and then transferred to PVDF membranes. After blocking with 5% skimmed milk for 1 h at room temperature, the membranes were incubated overnight at 4˚C with rabbit anti-MMP-2 (1:1,000; no. ab92536; Abcam), rabbit anti-MMP-9 (1:1,000; no. ab76003; Abcam), rabbit anti-TIMP-1 (1:1,000; no. ab211926; Abcam), rabbit anti-integrin β1 (1:1,000; no. ab52971; Abcam), rabbit anti-α-tubulin (1:5,000; no. ab18207; Abcam), rabbit anti-acetyl-α-tubulin (1:1,000; no. ab179484; Abcam) and rabbit anti-β-actin (1:5,000; no. ab8227; Abcam) antibodies. After three washes with TBS with 0.1% Tween-20, the immunoblots were incubated for 1 h at room temperature with goat alkaline phosphatase-labeled anti-rabbit antibody (1:1,000; cat. no. 14708; Cell Signaling Technology, Inc.). The immunoreactive bands were visualized using an enhanced chemiluminescence reagent (Beyotime Institute of Biotechnology). The blots were semi-quantified using ImageJ software (version 1.47; National Institutes of Health).

Cell transfection. miR-29b-3p mimic (50 nM; 5'-UAGCAC CAUUUGAAAUCAGUGUU-3'), NC mimics (50 nM; 5'-UUGUACUACACAAAAGUACUG-3'), miR-29b-3p inhibitor (100 nM; 5'-UUCUCCGAACGUGUCACGUTT-3'), NC inhibitor (100 nM; 5'-CAGUACUUUUGUGUAGUA-3'), specific small interfering RNAs (siRNAs) targeting MMP-9 (si-MMP-9; 1.0 μg; 5'-ACCACAACATCACCTATTGGA TC-3'), siRNA-negative control (si-NC; 1.0 μg; 5'-UUCUCC GAACGUGUCACGUTT-3') were purchased from Shanghai GenePharma Co., Ltd. To overexpress MMP-9, the sequences of MMP-9 were inserted into a pcDNA3.1 plasmid to obtain the MMP-9 overexpression plasmid pcDNA3.1-MMP-9 (OE-MMP-9; 1.0 μg; Shanghai GenePharma Co., Ltd.), and an empty pcDNA3.1 plasmid was used as the negative control (OE-NC; 1.0 μg). Plasmid DNA, siRNA, miR-mimic or miR-inhibitor was transfected into L-PHNECs, H-PHNECs or NP69 cells ($1x10^5$), which were subcultured at a density of 80%, with Lipofectamine® 2000 reagent (Invitrogen; Thermo Fisher Scientific, Inc.) at 37˚C. After transfection for 48 h, the transfection efficiency was detected via RT-qPCR and western blotting, and then subsequent experiments were performed.

Lipopolysaccharide (LPS) stimulation. NP69 cells ($1x10^5$ cells/well) were seeded in 12-well plates and transfected as described above. When the NP69 cells reached 80-90% confluence, the cells were washed with phosphate-buffered saline (PBS; 37˚C, pH 7.4), and fresh culture medium was added, along with LPS (Sangon Biotech Co., Ltd.) at a concentration of 1 μg/ml and incubated at 37˚C for 48 h.

Bioinformatics and luciferase reporter assays. StarBase (Version 2.0; http://starbase.sysu.edu.cn/) online software was used to predict the binding sites of miRNAs to target mRNAs. pmirGLO-MMP-9-wild-type (WT)/mutant (Mut) and pmirGLO-MMP-2-WT/Mut reporter plasmids were provided by Shanghai GenePharma Co., Ltd. 293T cells ($2x10^5$/well) were co-transfected with pmirGLO-MMP-9-Wt/Mut or pmirGLO-MMP-2-Wt/Mut plasmid (1.0 μg) and NC mimic or miR-29b-3p mimic (50 nM) using Lipofectamine® 2000 reagent at 37˚C. At 48 h post-transfection, luciferase activity was determined using the dual-luciferase reporter assay system (Promega Corporation). Firefly luciferase activities were normalized to *Renilla* luciferase activities.

Immunofluorescence staining. For immunofluorescence staining, 10-μm-thick tissue sections of CRSwNPs samples were fixed with 4% paraformaldehyde for 2 h at 4˚C. CRSwNPs were incubated with blocking solution [5% bovine serum albumin (Thermo Fisher Scientific, Inc.) with 0.2% Triton X-100] for 1 h at room temperature, and incubated overnight at 4˚C with antibodies against MMP-9 (1:500; cat. no. ab76003; Abcam) and integrin β1 (1:100; cat. no. ab52971; Abcam). After washing, the sections were incubated with Alexa Fluor 555-conjugated anti-rabbit IgG (1:500; no. ab150062; Abcam) at room temperature for 1 h, and the nuclei were counterstained with 4',6-diamidino-2-phenylindole (DAPI) for 30 min at room temperature. Fluorescence images were collected with a Nikon Eclipse 80i microscope (Nikon Corporation).

Co-immunoprecipitation (Co-IP) assays. Myc-integrin β1, Myc-α-tubulin and/or MMP-9-WT-HA plasmids were purchased from Transomic Technologies, Inc., and were transiently transfected into 293T cells with Lipofectamine® 2000 reagent (Invitrogen; Thermo Fisher Scientific, Inc.) at 37˚C. At 24 h posttransfection, the cells were harvested and lysed with 500 μl IP lysis buffer containing protease inhibitor cocktail (Thermo Fisher Scientific, Inc.). After incubating on ice for 5 min, the cell lysates were centrifuged (4˚C) at 13,000 x g for 10 min. Then, ~25% of the supernatant was subjected to input assays, and the remaining supernatant was used for the Co-IP assay with an anti-HA agarose affinity gel (Shanghai Yeasen Biotechnology Co., Ltd.) according to the manufacturer's instructions. Rabbit anti-HA (1 μg; cat. no. ab9110; Abcam) and rabbit anti-Myc (1 μg; cat. no. ab9106; Abcam) were used for IP. Beads alone were used as the negative control. Briefly, 500 μl agarose affinity gel was centrifuged at 13,000 x g for 30 sec at 4˚C to remove the glycerol and washed with cold TBS. Then, 500 μl cell lysate was added to the equilibrated resin and rocked gently on a rotating platform for 2 h at 4˚C. The resin was washed with cold TBS, and the protein samples were evaluated by western blotting.

GST-pull down assays. GST pull-down assays were carried out as previously described (34). Briefly, the pGEX-GST-MMP-9 plasmid was transformed into BL21 cells to GST-MMP-9 proteins. The pcDNA-Myc-integrin β1 or pcDNA-Myc-α-tubulin plasmid was transfected into 293T cells to express Myc-integrin β1 and Myc-α-tubulin proteins. The Pierce™ GST Protein Interaction Pull-Down Kit (cat. no. 21516; Pierce; Thermo Fisher Scientific, Inc.) was used according to the manufacturer's instructions. BL21 cells expressing GST-MMP-9 proteins were treated with pull-down lysis buffer and immobilized on equilibrated glutathione agarose resin at 4˚C for 2 h. The resin was washed with wash solution (TBS with Pull-down lysis buffer), and 293T lysates containing Myc-integrin β1 or Myc-α-tubulin protein were added, followed by incubation at 4˚C for 12 h. After washing

with a wash solution (TBS with Pull-down lysis buffer), the resin was eluted with glutathione elution buffer. The protein samples were evaluated via western blotting.

Cell viability assays. After 24 h of treatment with 1 μg/ml LPS, cell viability was assessed using Cell Counting Kit-8 (CCK-8; Beyotime Institute of Biotechnology). Briefly, cells were seeded in 96-well plates at a density of $1x10^5$ cells/well; 10 μl CCK-8 solution was added to each well and incubated for 4 h. The OD value at 450 nm was measured utilizing a microplate reader (BioTek Instruments, Inc.).

Detection of cell apoptosis. Apoptosis was detected using an Annexin V combined fluorescein isothiocyanate (FITC)/propidine iodide (PI) cell apoptosis detection kit (Beijing Solarbio Science & Technology Co., Ltd.). In brief, cells were collected using cold PBS buffer and then cultured with 5 μl Annexin V-FITC reagent and 5 μl PI in the dark for 15 min at room temperature. Subsequently, 400 μl 1X binding buffer was added, and the cells were analyzed using a BD FACSCanto II flow cytometer (BD Biosciences) with FlowJo software (version 10; FlowJo LLC). Early and late apoptosis were both analyzed.

ELISA. The cell culture media was centrifuged at 2,000 x g for 10 min to remove debris, and the cell-free culture supernatants were collected after treatment. The secretory levels of IL-6 (cat. no. 900-T16), TNF-α (cat. no. 900-M25) and IL-1β (cat. no. 900-M95) were analyzed using their corresponding ELISA kits (PeproTech China.) according to the manufacturer's protocol. The concentrations of inflammatory cytokines were measured using a microplate spectrophotometer (BioTek Instruments, Inc.) at a wavelength of 450 nm.

miR-29b-3p differential analysis by Gene Expression Omnibus (GEO). Differential expression of miR-29b-3p between three nasal cell samples and four nasal polyps cell samples from airway epithelia samples was analyzed using the NCBI GEO DataSets portal: http://www.ncbi.nlm.nih.gov/geo/. The miRNA expression data (GEO accession no. GSE159708) from high-throughput sequencing were submitted by Pommier *et al* (35). The web-accessible analysis tool GEO2R (https://www.ncbi.nlm.nih.gov/geo/geo2r/) was utilized on its default settings to screen the miR-29b-3p expression of each dataset. The cut-off value for the filtration criteria was set at FDR<0.05 and log2 fold-change>1.

Bivariate correlation analysis. In the 100 CRSwNPs tissue samples, the levels of MMP-2, MMP-9 and TIMP-1 protein were detected via western blotting, the blots were semi-quantified by ImageJ software and normalized to those of the internal reference gene β-actin. The levels of miR-29b-3p were determined via RT-qPCR, and the relative expression levels were calculated using the $2^{-\Delta\Delta Cq}$ method and normalized to those of internal reference gene U6. Bivariate correlation analyses of the correlations between MMP-2 and MMP-9 expression and miR-29b-3p, or TIMP-1 expression were performed.

Statistical analysis. All the experiments were repeated three times. GraphPad Prism 8 (GraphPad Software, Inc.) was used for statistical analysis, and the data are presented as the mean ± standard deviation. Data between two groups were analyzed using an unpaired Student's t-test, and data among multiple groups were analyzed by one-way analysis of variance (ANOVA) followed by a Tukey's post hoc test. P<0.05 was considered to indicate a statistically significant difference.

Results

Correlations between miR-29b-3p, MMP-2, MMP-9 and TIMP-1 expression in CRSwNPs. Previous studies have shown that miR-29b-3p regulates the expression of MMP-2 and MMP-9 (28,29), and the balance between MMPs and TIMPs is important in tissue homeostasis within CRSwNPs (5). To examine the relationships between miR-29b-3p, MMP-2/MMP-9 and TIMP-1 in CRSwNPs, the mRNA expression of miR-29b-3p was detected using RT-qPCR, and the protein expression levels of MMP-2, MMP-9 and TIMP-1 were determined via western blotting in 100 CRSwNPs tissue samples (Fig. S1). The results showed that miR-29b-3p expression was moderately positively correlated with the expression of MMP-2 (r=0.4420; P<0.001; Fig. 1A) and MMP-9 (r=0.4799; P<0.001; Fig. 1B), and TIMP-1 expression was moderately negatively correlated with the expression of MMP-2 (r=-0.4672; P<0.001; Fig. 1C) and MMP-9 (r=-0.4484; P<0.001; Fig. 1D). Immunofluorescent images showed MMP-2, MMP-9 and TIMP-1 protein expression in CRSwNPs tissue samples (Fig. 1E). These observations suggested that miR-29b-3p plays a protective role in the regulation of the balance in MMP and TIMP expression.

miR-29b-3p targets MMP-2 and MMP-9 in PHNECs. Previous studies have shown that miR-29b-3p targets the 3'-untranslated region of MMP-2 and MMP-9 (28,29). Using the bioinformatics database StarBase to search for potential targets, a putative interaction between miR-29b-3p and MMP-2/MMP-9 was found, and the target binding sequence is shown in Fig. 2A and B. A dual-luciferase reporter assay demonstrated that MMP-2-WT/MMP-9-WT and miR-29b-3p mimic co-transfection significantly decreased the luciferase activities in 293T cells (P<0.01; Fig. 2C and D), while MMP-2-MUT/MMP-9-MUT and miR-29b-3p mimic co-transfection failed to affect the luciferase activity in 293T cells (P>0.05; Fig. 2C and D). Next, transfection of miR-29b-3p inhibitor and miR-29b-3p mimic into PHNECs significantly decreased and increased miR-29b-3p expression, respectively (P<0.01; Fig. 2E and G). Notably, transfection of miR-29b-3p inhibitor into PHNECs significantly increased MMP-2 and MMP-9 protein expression in L-PHNECs (P<0.01; Fig. 2F), and transfection with miR-29b-3p mimic significantly decreased MMP-2 and MMP-9 protein expression in H-PHNECs (P<0.01; Fig. 2H). Altogether, the aforementioned results indicated that miR-29b-3p directly targeted both the MMP-2 and MMP-9 genes.

MMP-9 binds to integrin b1. Compared with MMP-2, the r value (Fig. 1A and B) and the targeting capability (Fig. 2F and H) were higher for MMP-9. Thus, the miR-29b-3p/MMP-9 axis was investigated in subsequent assays. In a recent study, integrin β1 and α-tubulin were identified as potential MMP-9-interacting proteins (25). To examine

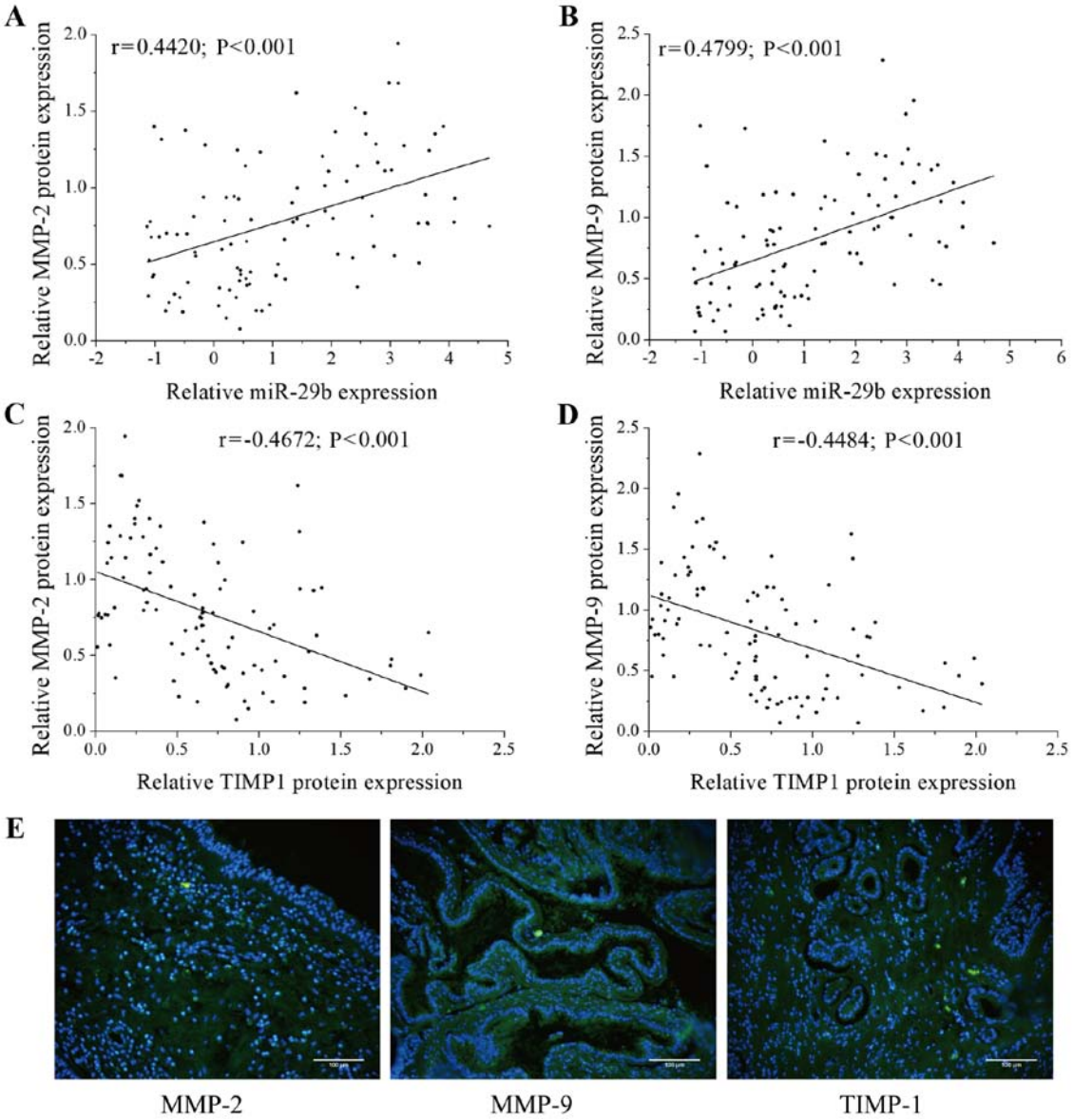

Figure 1. Correlation between miR-29b-3p, MMP-2, MMP-9 and TIMP-1 expression in CRSwNPs. Correlation between miR-29b-3p expression and (A) MMP-2 and (B) MMP-9 expression in CRSwNPs samples (n=100). The X-axis represents the expression of miR-29b-3p, the Y-axis represents the expression of MMP-2/MMP-9, each point in the figure represents a sample, and the P-value and the correlation coefficient (r value) are stated. The data were normalized to U6 expression and are shown as the Cq value. Correlation between TIMP-1 expression and (C) MMP-2 and (D) MMP-9 expression in CRSwNPs samples (n=100). The X-axis represents the expression of TIMP-1, the Y-axis represents the expression of the MMP-2/MMP-9, each point in the figure represents a sample, and the P-value and the correlation coefficient (r value) are stated. (E) The expression of MMP-2, MMP-9 and TIMP-1 based on immunofluorescence staining. Green staining shows positive expression of MMP-2, MMP-9 and TIMP-1, and blue (DAPI) indicates nuclear staining. Scale bar, 100 μm. miR, microRNA; MMP, matrix metalloproteinase; TIMP-1, tissue inhibitor of metalloproteinase 1; CRSwNPs, chronic rhinosinusitis with nasal polyps.

the interaction between MMP-9 and integrin β1/α-tubulin, Myc-integrin β1/Myc-α-tubulin and HA-MMP-9 were transiently co-expressed in 293T cells and Co-IP assays were performed using a HA antibody. Indeed, MMP-9 readily immunoprecipitated Myc-tagged integrin β1 and α-tubulin (Fig. 3A and B). To further determine whether the interaction between integrin β1/α-tubulin and MMP-9 was direct, GST pull-down assays were performed using the GST-MMP-9 protein expressed in and purified from bacteria. As shown in Fig. 3C and D, GST-fused MMP-9 pulled down integrin β1, but not α-tubulin. These observations suggested that integrin β1 could directly interact with MMP-9, but that α-tubulin indirectly interacts with MMP-9. These results suggested that MMP-9 binds with integrin β1.

miR-29b-3p affects the acetyl-α-tubulin levels by increasing MMP-9 and integrin b1 binding. MMP-9 and integrin β1 activation can increase α-tubulin acetylation (23), and Smith (24) and the present study found that MMP-9 directly bound to integrin β1 (Fig. 3C). We hypothesized that MMP-9 binds to integrin β1 to promote α-tubulin acetylation by down-regulating miR-29b-3p in CRSwNPs. MMP-9 expression was knocked down in H-PHNECs by transfection with si-MMP-9 (P=0.024; Fig. 4A), whereas expression of MMP-9 was upregulated in L-PHNECs by transfection with OE-MMP-9 (P<0.01; Fig. 4B). To test this hypothesis, miR-29b-3p was overexpressed in H-PHNECs. The western blotting results showed that MMP-9 expression was reduced after overexpression of miR-29b-3p (P<0.01), but this effect was reversed after

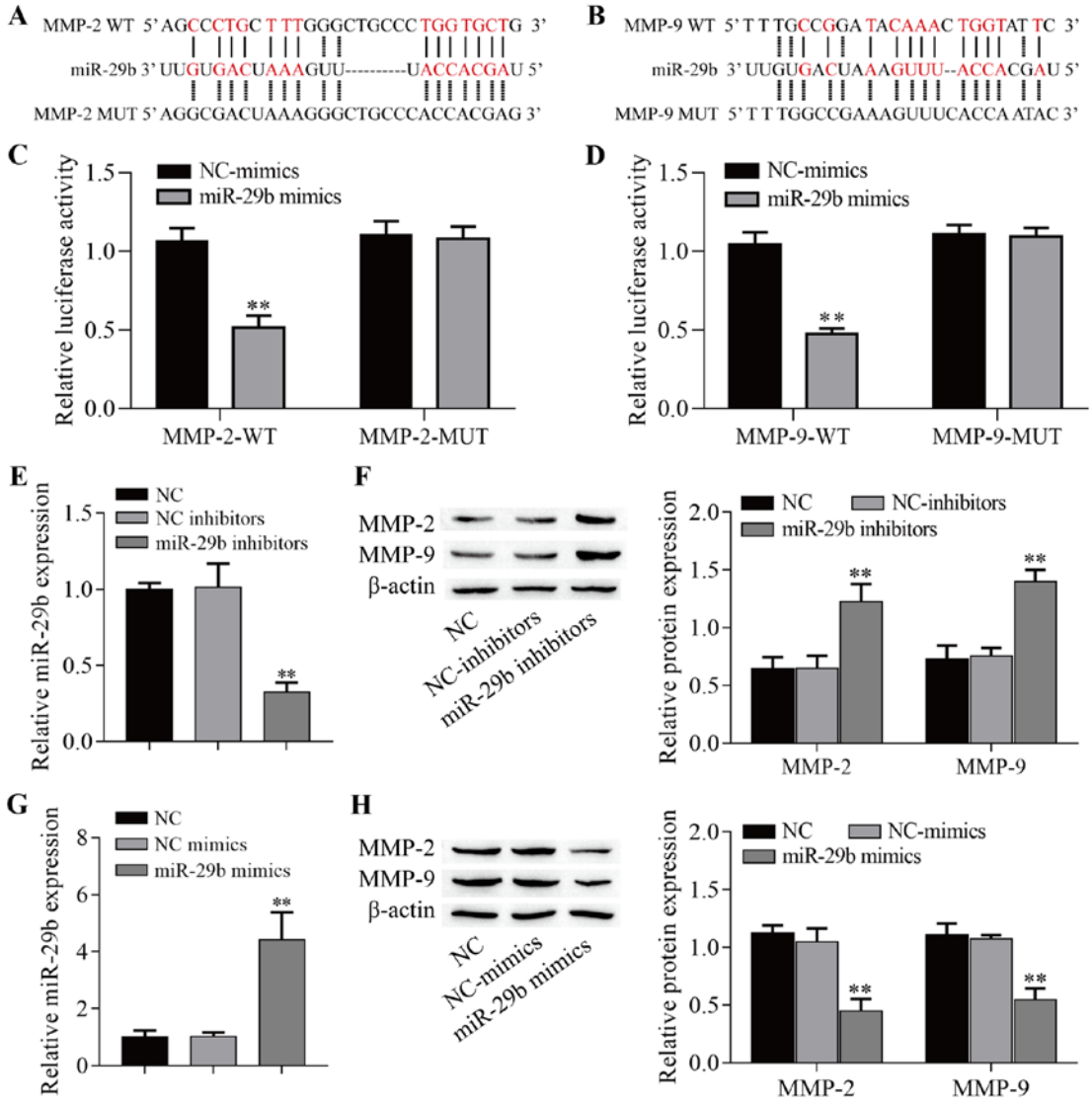

Figure 2. miR-29b-3p targets MMP-2 and MMP-9 in chronic rhinosinusitis with nasal polyps. (A and B) Schematic image of the binding site of miR-29b-3p and MMP-2-WT/MMP-9-WT and the binding site of MMP-2-MUT/MMP-9-MUT. Dual-luciferase reporter assays were used to show that miR-29b-3p can target (C) MMP-2 and (D) MMP-9 in 293T cells. **P<0.01 vs. NC mimics. (E) Transfection of miR-29b-3p inhibitors significantly decreased miR-29b-3p expression in L-PHNECs cells (n=3). (F) Transfection of miR-29b-3p inhibitors significantly increased MMP-2 and MMP-9 expression in L-PHNECs cells (n=3). (G) Transfection of miR-29b-3p mimics significantly increased miR-29b-3p expression in H-PHNECs cells (n=3). (H) Transfection of miR-29b-3p mimics significantly decreased MMP-2 and MMP-9 expression in H-PHNECs cells (n=3). **P<0.01 vs. NC group. L-PHNECs, PHNECs with the lowest MMP-2 and MMP-9 expression; H-PHNECs, PHNECs with highest MMP-2 and MMP-9 expression; miR, microRNA; MMP, matrix metalloproteinase; NC, negative control; WT, wild-type; MUT, mutant type.

overexpression of MMP-9 (P<0.01; Fig. 4C). By contrast, the expression of acetyl-α-tubulin was elevated after overexpression of miR-29b-3p (P<0.01), which was repressed by overexpression of MMP-9 (P<0.01). In addition, miR-29b-3p expression was inhibited in L-PHNECs. These results showed the expression of MMP-9 was elevated by miR-29b-3p inhibitors (P<0.01), but this effect was reversed by MMP-9 knockdown (P=0.002; Fig. 4D). By contrast, the expression of acetyl-α-tubulin was decreased by the inhibition of miR-29b-3p (P<0.01), but it was enhanced by MMP-9 knockdown. Of note, the protein expression of integrin β1 was not affected (P>0.05). Immunofluorescence was performed to examine the protein expression of MMP-9 and integrin β1 in tissues with lower and higher MMP-9 expression. As shown in Fig. 4E, there was no notable difference in the expression of integrin β1 in low and high MMP tissues. Next, the correlation between MMP-9 and acetyl-α-tubulin expression was further analyzed in 100 CRSwNPs tissue samples, and a moderate negative correlation was observed between MMP-9 and acetyl-α-tubulin (r=-0.3435; P=0.004; Fig. 4F). Taken together, we propose a novel model in which MMP-9 binds to integrin β1 to promote α-tubulin deacetylation-mediated tissue remodeling by downregulating miR-29b-3p in CRSwNPs (Fig. 4G).

miR-29b-3p regulates LPS-induced viability, apoptosis and inflammation of NP69 cells by targeting MMP-9. MMP-9 expression was downregulated in NP69 cells by transfection with si-MMP-9 (P=0.043; Fig. 5A), whereas expression was upregulated by transfection with OE-MMP-9 (P=0.006; Fig. 5B). To explore the potential role of miR-29b-3p in CRSwNPs, miR-29b-3p expression in nasal polyps was investigated using the GEO database. This analysis showed

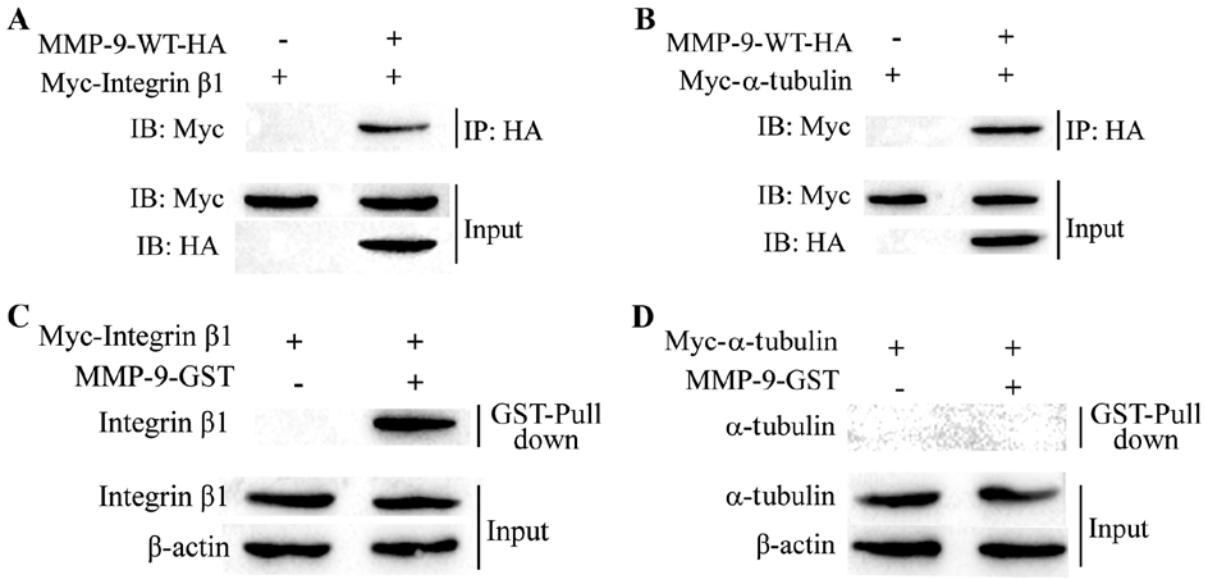

Figure 3. MMP-9 binds to integrin β1. For the co-immunoprecipitation assay, cells were transfected with (A) pcDNA-Myc-integrin β1 or (B) pcDNA-Myc-α-tubulin for 24 h. The transfected cells were lysed and immunoprecipitated, and western blot analysis was conducted using anti-Myc and anti-MMP antibodies. In the GST pull-down assay, the GST-MMP-9 fusion protein expressed in BL21 cells was purified with glutathione agarose resin and incubated with lysates of (C) Myc-integrin β1- or (D) Myc-α-tubulin-expressing cells. Western blot analysis was performed using anti-integrin β1, anti-α-tubulin, anti-Myc and β-actin antibodies. MMP, matrix metalloproteinase.

that miR-29b-3p was expressed at lower levels in nasal polyps (P=0.008; Fig. 5C). Next, miR-29b-3p expression in PHNECs and NP69 cells was measured via RT-qPCR. As shown in Fig. 5D, the expression of miR-29b-3p was downregulated in both L-PHNECs and H-PHNECs compared with NP69 cells (P<0.001), and it was expressed at lower levels in H-PHNECs than in L-PHNECs (P=0.005). These results suggested that miR-29b-3p was downregulated in CRSwNPs. Next, a cell model of LPS-induced CRSwNPs was investigated. The results showed that miR-29b-3p expression was significantly lower in LPS-induced NP69 cells than in the control cells (P<0.01; Fig. 5E) and was significantly increased by the upregulation of miR-29b-3p compared with the LPS group (P<0.01). Notably, overexpression of MMP-9 reduced miR-29b-3p expression compared with the LPS + miR-29 mimics group (P<0.01) and knockdown of MMP-9 elevated miR-29b-3p expression compared with the LPS group (P<0.01). In addition, LPS also significantly increased MMP-9 expression in NP69 cells (P<0.01; Fig. 5F), which were effectively reversed by upregulation of miR-29b-3p and knockdown of MMP-9 (P<0.01), whereas overexpression of MMP-9 reversed the inhibitory effect of miR-29b-3p upregulation (P<0.01). Conversely, LPS significantly decreased acetyl-α-tubulin level (P<0.01; Fig. 5F), which was effectively elevated by upregulation of miR-29b-3p and knockdown of MMP-9 (P<0.05), but overexpression of MMP-9 reversed the effects of miR-29b-3p overexpression (P<0.01). Of note, the protein expression of integrin β1 was not altered (P>0.05). The results suggested that miR-29b-3p regulated acetyl-α-tubulin levels by targeting MMP-9. Next, cell viability, apoptosis and inflammatory cytokines (IL-1β, IL-6 and TNF-α) of LPS-induced NP69 cells were determined. As presented in Fig. 5G, cell viability was inhibited after LPS induction (P<0.01), and upregulation of miR-29b-3p and knockdown of MMP-9 alleviated the inhibitory effect of LPS (P<0.01). Overexpression of MMP-9 reduced the alleviatory effect of miR-29b-3p upregulation on cell viability (P<0.01). Moreover, cell apoptosis and inflammatory cytokine levels were increased after LPS induction (P<0.01; Fig. 5H and I), and these effects were reduced by the upregulation of miR-29b-3p and knockdown of MMP-9 (P<0.01); however, the overexpression of MMP-9 repressed the inhibitory effect of miR-29b-3p upregulation (P<0.01). These data indicated that overexpression of miR-29b-3p alleviated LPS-induced inflammation in NP69 cells by targeting MMP-9.

Discussion

Ciliogenesis and cilia function are significantly impaired in the CRSwNPs epithelium, presumably due to the altered expression of miRNAs (30). The function of miRNAs in CRSwNPs remains unclear. In previous reports, miR-29b-3p was shown to directly and indirectly regulate MMP-2 and MMP-9 expression (28,29). It is commonly known that MMPs are likely to be associated with airway remodeling in CRSwNPs based on the increased expression of MMP-2 and MMP-9 in patients with CRSwNPs compared with control subjects (36-38). Numerous studies have found that the levels of MMPs are significantly increased in CRSwNPs compared with healthy control tissues and that the levels of TIMPs are significantly decreased (10-13). In the present study, no healthy samples were analyzed as a control group, so it cannot be concluded that the expression levels of MMP-2, MMP-9, TIMP-1 and miR-29b-3p differ in CRSwNPs compared with healthy individuals. However, it was found that TIMP-1 expression was negatively correlated with the expression of MMP-2 and MMP-9 (Fig. 1C and D), and the results suggested that the imbalance in MMPs and TIMPs is closely associated with the development of CRSwNPs. In addition, miR-29b-3p expression was positively correlated with the expression of MMP-2

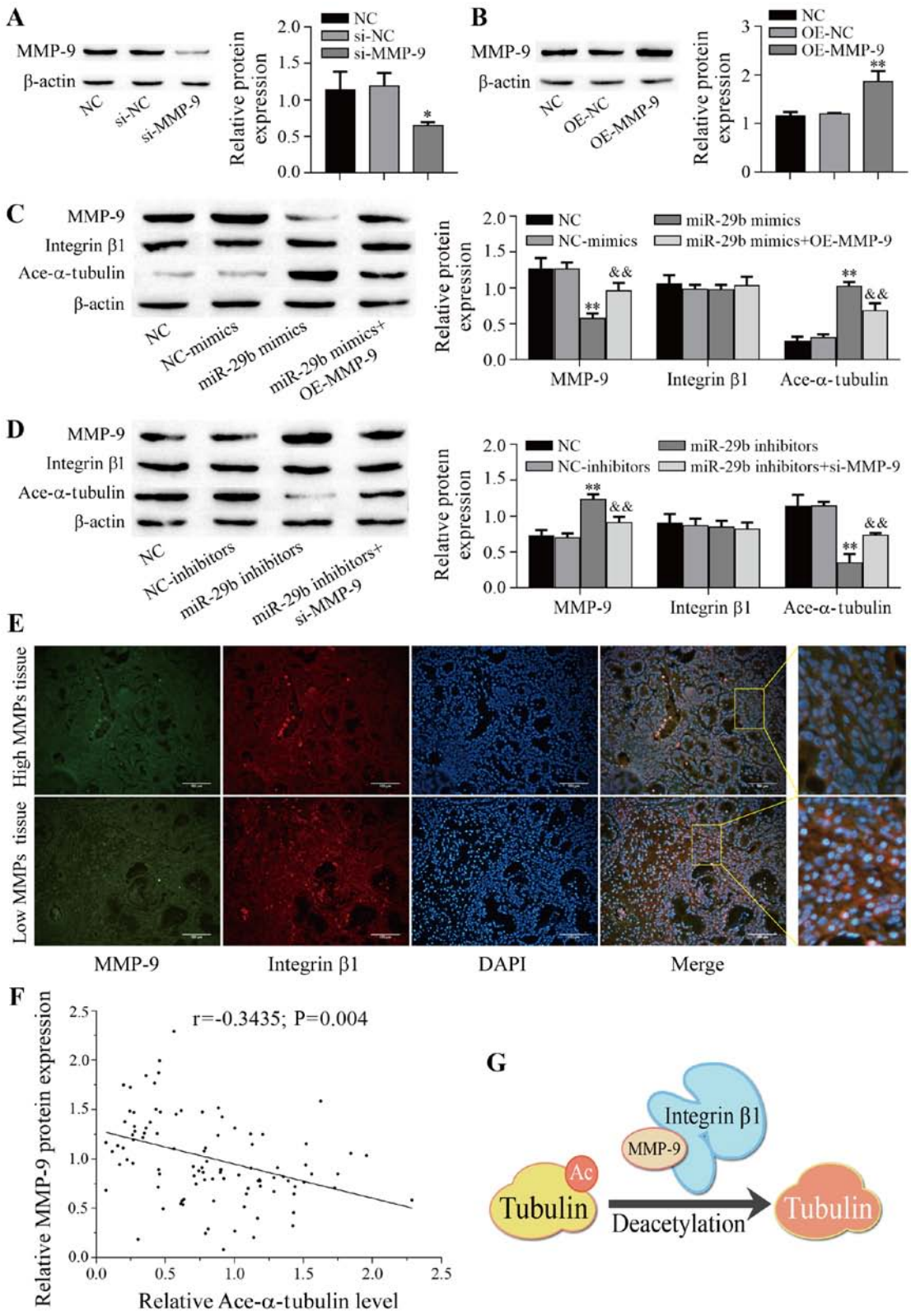

Figure 4. miR-29b-3p affects the acetyl-α-tubulin levels by increasing the MMP-9 and integrin β1 binding in CRSwNPs. (A-D) Protein expression was detected via western blotting (n=3). (E) The expression of MMP-9 and integrin β1 was determined by immunofluorescence staining. Green indicates positive expression of MMP-9, red indicates positive expression of integrin β1, and blue (DAPI) indicates nuclear staining. Scale bar, 100 μm. (F) Correlation between MMP-9 expression with acetyl-α-tubulin expression in CRSwNPs samples (n=100). The X-axis represents the expression of acetyl-α-tubulin, the Y-axis represents the expression of MMP-9, each point in the figure represents a sample, and the P-value and the correlation coefficient (r value) are stated. (G) Working model showing that MMP-9 binds to integrin β1 to promote α-tubulin deacetylation. *P<0.05, **P<0.01 vs. NC; $^{\&\&}$P<0.01 vs. miR-29b inhibitors or miR-29b mimics. miR, microRNA; MMP, matrix metalloproteinase; CRSwNPs, chronic rhinosinusitis with nasal polyps; NC, negative control; si-, small interfering RNA; OE, overexpression vector.

and MMP-9 in CRSwNPs (Fig. 1A and B), and miR-29b-3p directly targeted both the MMP-2 and MMP-9 genes (Fig. 2). Chen *et al* (28) found that oxidized low-density lipoprotein upregulates miR-29b-3p and increases MMP-2 and MMP-9

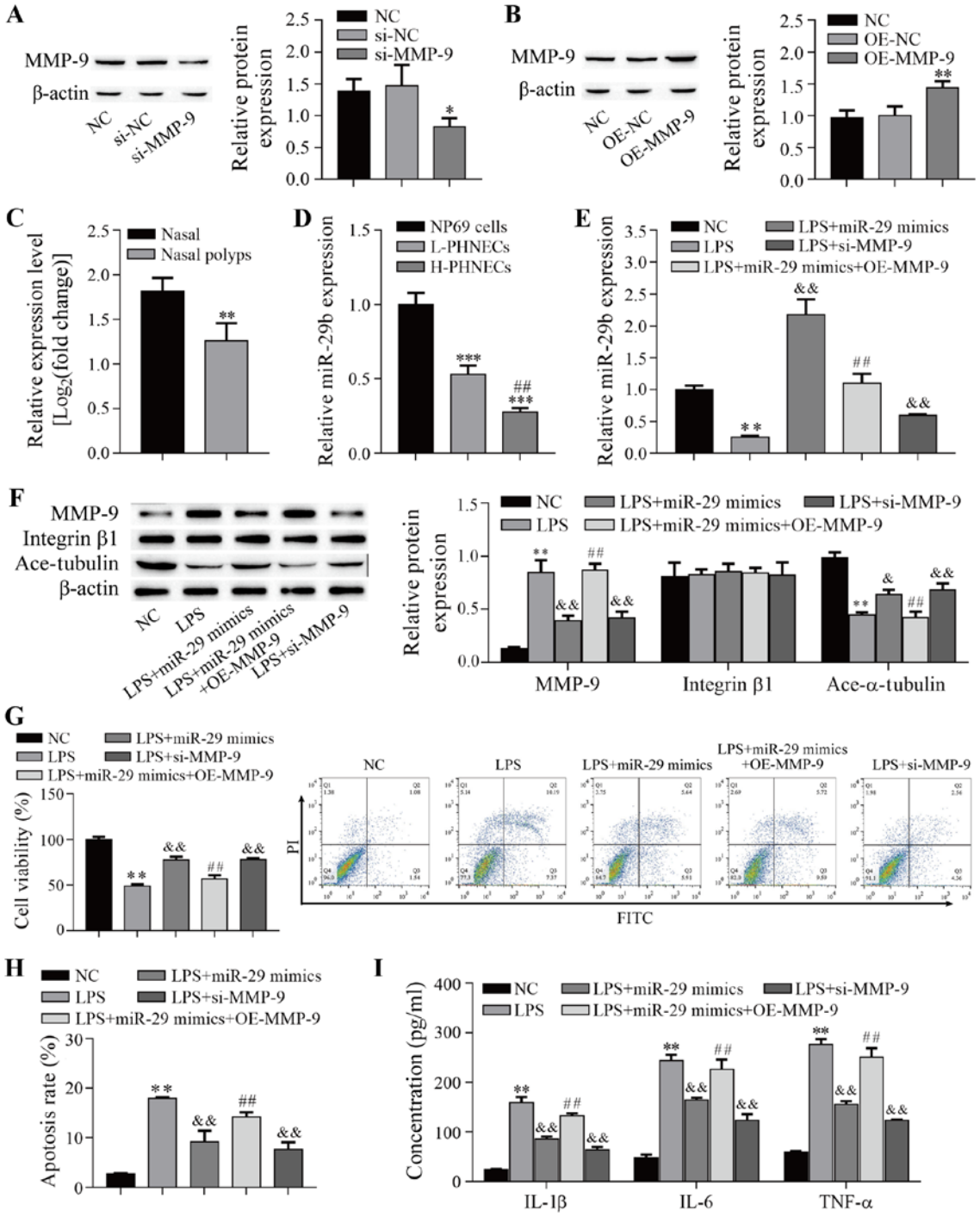

Figure 5. miR-29b-3p alleviates LPS-induced inflammation in NP69 cells by targeting MMP-9. (A and B) Protein expression was detected via western blotting (n=3). (C) The expression of miR-29b-3p was downregulated in the nasal polyps cells (n=4) compared with nasal cells (n=3) from airway epithelia samples. The GEO2R analysis tool was used to analyze the miRNA expression dataset (GEO accession no. GSE159708) to screen the miR-29b-3p expression of each dataset. The cut-off value for the filtration criteria was set at FDR <0.05 and log2 fold-change >1. **P<0.01 vs. Nasal. (D) The expression of miR-29b-3p was downregulated in both L-PHNECs and H-PHNECs compared with NP69 cells (n=3). ***P<0.001 vs. NP69 cells; $^{\#\#}$P<0.01 vs. L-PHNECs. (E) LPS treatment decreased miR-29b-3p expression (n=3). (F) Protein expression was determined via western botting (n=3). (G) Cell viability was determined via Cell Counting Kit-8 assay (n=3). (H) Cell apoptosis was determined by flow cytometry (n=3). (I) The inflammatory cytokine levels were determined by ELISA (n=3). *P<0.05, **P<0.01 vs. NC; $^{\&}$P<0.05, $^{\&\&}$P<0.01 vs. LPS; $^{\#\#}$P<0.01 vs. LPS + miR-29b mimics. L-PHNECs, PHNECs with the lowest MMP-2 and MMP-9 expression; H-PHNECs, PHNECs with highest MMP-2 and MMP-9 expression; miR/miRNA, microRNA; LPS, lipopolysaccharide; MMP, matrix metalloproteinase; NC, negative control; GEO, Gene Expression Omnibus; si-, small interfering RNA; OE, overexpression vector.

expression by reducing DNA methylation in cardiovascular diseases. Of note, a recent study showed that MMP-2 and MMP-9 were target genes of miR-29b-3p, and metformin alleviates polycystic ovary syndrome by decreasing the expression of MMP-2 and MMP-9 via upregulation of miR-29b-3p expression (29). Thus, bioinformatics analysis and luciferase activity assays identified MMP-2 and MMP-9 as functional targets of miR-29b-3p in CRSwNPs.

In the present study, it was found that LPS treatment increased MMP-9 expression (Fig. 5F) and that overexpression

of miR-29b-3p alleviated LPS-induced inflammation in NP69 cells by targeting MMP-9 (Fig. 5I). This study further demonstrated that the miR-29b-3p/MMP-9 axis may regulate remodeling in CRSwNPs. A recent study showed that MMP-9 and integrin activity both regulate fibroblast migration by increasing α-tubulin acetylation (23), which can directly bind to integrins to activate signaling, which involves cell adhesion molecules and pro-forms of growth factors (24). Previous studies have shown that the hemopexin domain of MMP-9 can interact with different integrin subunits to promote enhanced cancer cell migration, invasion and proliferation in various cancer cell types, such as colon cancer cells, B cell chronic lymphocytic leukemia and breast cancer cells (39-42). Notably, the integrin β1, Src, elongation factor 1-α 2, α-tubulin, actin and histone H2B proteins are potential MMP-9-interacting proteins (25). In the present study, it was shown that integrin β1 and MMP-9 bind directly (Fig. 3A and C), but α-tubulin and MMP-9 indirectly interact (Fig. 3B and D). Furthermore, overexpression and knockdown of MMP-9 did not just alter MMP-9 expression, but, as a novel finding, it also altered α-tubulin acetylation levels (Fig. 4C and D). However, overexpression and knockdown of MMP-9 failed to regulate integrin β1 expression (Fig. 4C and D). In addition, a moderate negative correlation between MMP-9 and acetyl-α-tubulin expression levels was also found (Fig. 4F). Our observations demonstrated that MMP-9-integrin β1 complexes promoted α-tubulin deacetylation (Fig. 4G). Of note, this result contrasts with Lee *et al* (23), who found that MMP-9 and integrin activation can increase α-tubulin acetylation. Previous research suggests that integrins inhibit the activation of histone deacetylase 6 by activating AKT signaling, which then suppresses acetyl-α-tubulin deacetylation (43,44). We hypothesize that MMP-9 binds to integrin β1 to promote acetyl-α-tubulin deacetylation by inhibiting the activation of integrin signaling. Each integrin is a heterodimer composed of an α- and a β-subunit and must be assembled as a heterodimer within the endoplasmic reticulum in order to be expressed on the cell surface (45). Thus, we speculate that MMP-9 binds to integrin αβ1 homodimers to promote acetyl-α-tubulin deacetylation. These are all areas of interest that we will continue to investigate in further studies.

Although the cellular mechanisms underlying the development of CRSwNPs remain uncertain, polyp formation occurs due to the protrusion of connective tissue through an initial epithelial defect and remodeling (46). The present study further demonstrated that MMP-9-integrin β1 complexes promote α-tubulin deacetylation involved in the airway remodeling of CRSwNPs. Few studies have investigated whether the acetylation of α-tubulin plays an important role in MT stabilization and cell morphology, and loss of α-tubulin acetylation is associated with epithelial-mesenchymal transition and chronic airway remodeling (21,22). In addition, inhibition of HDACs improves endothelial barrier function and attenuates the progression of osteoarthritis by suppressing α-tubulin deacetylation (47,48). In the present study, it was shown that the miR-29b-3p/MMP-9 axis decreased acetyl-α-tubulin levels and that overexpression of miR-29b-3p significantly decreased MMP-9 expression and increased the acetyl-α-tubulin levels in PHNECs. LPS-induced inhibition of acetyl-α-tubulin levels and overexpression of miR-29b-3p not only increased the acetyl-α-tubulin levels (Fig. 5F), but also alleviated LPS-induced inflammation in NP69 cells (Fig. 5I). Thus, targeting miR-29b-3p/MMP-9 is a novel strategy for the clinical treatment of CRSwNPs.

In conclusion, miR-29b-3p expression was positively correlated with the expression of MMP-2 and MMP-9 in CRSwNPs, and TIMP-1 expression was negatively correlated with the expression of MMP-2 and MMP-9. miR-29b-3p affects the acetyl-α-tubulin levels by increasing MMP-9 and integrin β1 interaction. The miR-29b-3p/MMP-9 pathway was identified as a novel protective axis in CRSwNPs and provided a significant theoretical foundation for developing novel therapies for CRSwNPs.

Acknowledgements

Not applicable.

Funding

This study was funded by the National Natural Science Foundation of China (NSFC; grant no. 81960187), Applied basic research of Yunnan Province [grant no. 2017FE468(-195)] and Scientific Research Fund of Yunnan Education Department (grant no. 2019J1262).

Availability of data and materials

The datasets used and/or analyzed during the present study are available from the corresponding author on reasonable request.

Authors' contributions

ZL designed the study, performed the experiments, and prepared and revised the final manuscript. HL designed the study, collected the clinical samples, analyzed and interpreted the data and revised the final manuscript. DY performed the experiments, commented on the data analysis and revised the manuscript. JG performed the experiments, analyzed and interpreted the data, and finalized the manuscript. BR designed the study, and prepared and revised the final manuscript. RL designed the study, and prepared and revised the final manuscript. BR and RL confirm the authenticity all the raw data. All the authors read and approved the final manuscript.

Ethics approval and consent to participate

All the experimental protocols were checked and approved by the Medical Ethics Committee of The First People's Hospital of Qujing (Qujing, China), and written informed consent was obtained from each patient before participation in the study.

Patient consent for publication

Not applicable.

Competing interests

The authors declare that they have no competing interests.

References

1. Sarig-Nadir O and Seliktar D: The role of matrix metalloproteinases in regulating neuronal and nonneuronal cell invasion into PEGylated fibrinogen hydrogels. Biomaterials 31: 6411-6416, 2010.
2. Fang CY, Zhang J, Yang HL, Peng LL, Wang K, Wang YJ, Zhao X, Liu HJ, Dou CH, Shi LH, *et al*: Leucine aminopeptidase 3 promotes migration and invasion of breast cancer cells through upregulation of fascin and matrix metalloproteinases-2/9 expression. J Cell Biochem 120: 3611-3620, 2019.
3. Gerwien H, Hermann S, Zhang X, Korpos E, Song J, Kopka K, Faust A, Wenning C, Gross CC, Honold L, *et al*: Imaging matrix metalloproteinase activity in multiple sclerosis as a specific marker of leukocyte penetration of the blood-brain barrier. Sci Transl Med 8: 364ra152, 2016.
4. Eifan AO, Orban NT, Jacobson MR and Durham SR: Severe persistent allergic rhinitis. Inflammation but no histologic features of structural upper airway remodeling. Am J Respir Crit Care Med 192: 1431-1439, 2015.
5. Kahveci OK, Derekoy FS, Yilmaz M, Serteser M and Altuntas A: The role of MMP-9 and TIMP-1 in nasal polyp formation. Swiss Med Wkly 138: 684-688, 2008.
6. Kelly EA, Busse WW and Jarjour NN: Increased matrix metalloproteinase-9 in the airway after allergen challenge. Am J Respir Crit Care Med 162: 1157-1161, 2000.
7. Chen Y, Peng W, Raffetto JD and Khalil RA: Matrix metalloproteinases in remodeling of lower extremity veins and chronic venous disease. Prog Mol Biol Transl Sci 147: 267-299, 2017.
8. Pinet K and McLaughlin K: Mechanisms of physiological tissue remodeling in animals: Manipulating tissue, organ, and organism morphology. Dev Biol 451: 134-145, 2019.
9. Alaseem A, Alhazzani K, Dondapati P, Alobid S, Bishayee A and Rathinavelu A: Matrix metalloproteinases: A challenging paradigm of cancer management. Semin Cancer Biol 56: 100-115, 2019.
10. Can IH, Ceylan K, Caydere M, Samim EE Ustun H and Karasoy DS: The expression of MMP-2, MMP-7, MMP-9, and TIMP-1 in chronic rhinosinusitis and nasal polyposis. Otolaryngol Head Neck Surg 139: 211-215, 2008.
11. Wang JH, Kwon HJ and Jang YJ: Staphylococcus aureus increases cytokine and matrix metalloproteinase expression in nasal mucosae of patients with chronic rhinosinusitis and nasal polyps. Am J Rhinol Allergy 24: 422-427, 2010.
12. Li X, Meng J, Qiao X, Liu Y, Liu F, Zhang N, Zhang J, Holtappels G, Luo B, Zhou P, *et al*: Expression of TGF, matrix metalloproteinases, and tissue inhibitors in Chinese chronic rhinosinusitis. J Allergy Clin Immunol 125: 1061-1068, 2010.
13. Guerra G, Testa D, Salzano F, Tafuri D, Hay E, Schettino BA, Iovine R, Marcuccio G and Motta G: Expression of matrix metalloproteinases and their tissue inhibitors in chronic rhinosinusitis with nasal polyps: Etiopathogenesis and recurrence. Ear Nose Yhroat J 145561319896635, 2020.
14. Yigit O, Acioğlu E, Gelişgen R, Server EA, Azizli E and Uzun H: The effect of corticosteroid on metalloproteinase levels of nasal polyposis. Laryngoscope 121: 667-673, 2011.
15. Wang C, Lou H, Wang X, Wang Y, Fan E, Li Y, Wang H, Bachert C and Zhang L: Effect of budesonide transnasal nebulization in patients with eosinophilic chronic rhinosinusitis with nasal polyps. J Allergy Clin Immunol 135: 922-929.e926, 2015.
16. Song Y and Brady S: Post-translational modifications of tubulin: Pathways to functional diversity of microtubules. Trends Cell Biol 25: 125-136, 2015.
17. Janke C and Bulinski JC: Post-translational regulation of the microtubule cytoskeleton: Mechanisms and functions. Nat Rev Mol Cell Biol 12: 773-786, 2011.
18. Wloga D and Gaertig J: Post-translational modifications of microtubules. J Cell Sci 123: 3447-3455, 2010.
19. Vo NT and Bols NC: Demonstration of primary cilia and acetylated α-tubulin in fish endothelial, epithelial and fibroblast cell lines. Fish Physiol Biochem 42: 29-38, 2016.
20. Lee CC, Cheng YC, Chang CY, Lin CM and Chang JY: Alpha-tubulin acetyltransferase/MEC-17 regulates cancer cell migration and invasion through epithelial-mesenchymal transition suppression and cell polarity disruption. Sci Rep 8: 17477, 2018.
21. Gu S, Liu Y, Zhu B, Ding K, Yao TP, Chen F, Zhan L, Xu P, Ehrlich M, Liang T, *et al*: Loss of α-Tubulin acetylation is associated with TGF-β-induced epithelial-mesenchymal transition. J Biol Chem 291: 5396-5405, 2016.
22. McGraw M, Rioux J, Garlick R, Rancourt R, White C and Veress L: From the cover: Impaired proliferation and differentiation of the conducting airway epithelium associated with bronchiolitis obliterans after sulfur mustard inhalation injury in rats. Toxicol Sci 157: 399-409, 2017.
23. Lee HN, Bosompra OA and Coller HA: RECK isoforms differentially regulate fibroblast migration by modulating tubulin post-translational modifications. Biochem Biophys Res Commun 510: 211-218, 2019.
24. Smith AC: A glitch in the matrix: Aberrant extracellular matrix proteolysis contributes to alcohol seeking. Biol Psychiatry 81: 900-902, 2017.
25. Yin L, Li FQ, Li J, Yang XR, Xie XY, Xue LY, Li YL and Zhang C: Chronic intermittent ethanol exposure induces upregulation of matrix metalloproteinase-9 in the rat medial prefrontal cortex and hippocampus. Neurochem Res 44: 1593-1601, 2019.
26. Wang W, Yang C, Wang X, Zhou LY, Lao GJ, Liu D, Wang C, Hu MD, Zeng TT, Yan L and Ren M: MicroRNA-129 and -335 promote diabetic wound healing by inhibiting sp1-Mediated MMP-9 expression. Diabetes 67: 1627-1638, 2018.
27. del Campo SEM, Latchana N, Levine KM, Grignol VP, Fairchild ET, Jaime-Ramirez AC, Dao TV, Karpa VI, Carson M, Ganju A, *et al*: MiR-21 enhances melanoma invasiveness via inhibition of tissue inhibitor of metalloproteinases 3 expression: In vivo effects of MiR-21 inhibitor. PLoS One 10: e0115919, 2015.
28. Chen KC, Wang YS, Hu CY, Chang WC, Liao YC, Dai CY and Juo SH: OxLDL up-regulates microRNA-29b, leading to epigenetic modifications of MMP-2/MMP-9 genes: A novel mechanism for cardiovascular diseases. FASEB J 25: 1718-1728, 2011.
29. Chen Z, Wei H, Zhao X, Xin X, Peng L, Ning Y, Wang YP, Lan YL and Zhang QH: Metformin treatment alleviates polycystic ovary syndrome by decreasing the expression of MMPand MMPvia H19/miRb and AKT/mTOR/autophagy signaling pathways. J Cell Physiol 234: 19964-19976, 2019.
30. Callejas-Díaz B, Fernandez G, Fuentes M, Martínez-Antón A, Alobid I, Roca-Ferrer J, Picado C, Tubita V and Mullol J: Integrated mRNA and microRNA transcriptome profiling during differentiation of human nasal polyp epithelium reveals an altered ciliogenesis. Allergy 75: 2548-2561, 2020.
31. Zhang T, Zhou Y, You B, You YW, Yan YB, Zhang J, Pei Y, Zhang W and Chen J: miR-30a-5p inhibits epithelial-to-mesenchymal transition by targeting CDK6 in nasal polyps. Am J Rhinol Allergy 35: 152-163, 2021.
32. Yang P, Chen S, Zhong G, Kong W and Wang Y: Agonist of PPAR-γ reduced epithelial-mesenchymal transition in eosinophilic chronic rhinosinusitis with nasal polyps via inhibition of high mobility group box 1. Int J Med Sci 16: 1631-1641, 2019.
33. Livak KJ and Schmittgen TD: Analysis of relative gene expression data using real-time quantitative PCR and the 2(-Delta Delta C(T)) method. Methods 25: 402-408, 2001.
34. Zhang L, Zhao D, Jin M, Song MZ, Liu SC, Guo KK and Zhang YM: Rab18 binds to classical swine fever virus NS5A and mediates viral replication and assembly in swine umbilical vein endothelial cells. Virulence 11: 489-501, 2020.
35. Pommier A, Varilh J, Bleuse S, Delétang K, Bonini J, Bergougnoux A, Brochiero E, Koenig M, Claustres M and Taulan-Cadars M: miRNA repertoires of cystic fibrosis ex vivo models highlight miR-181a and miR-101 that regulate WISP1 expression. J Pathol 253: 186-197, 2021.
36. Mudd P, Katial R, Alam R, Hohensee S, Ramakrishnan V and Kingdom T: Variations in expression of matrix metalloproteinase-9 and tissue inhibitor of metalloproteinase-1 in nasal mucosa of aspirin-sensitive versus aspirin-tolerant patients with nasal polyposis. Ann Allergy Asthma Immunol 107: 353-359, 2011.
37. Chen Y, Langhammer T, Westhofen M and Lorenzen J: Relationship between matrix metalloproteinases MMP-2, MMP-9, tissue inhibitor of matrix metalloproteinases-1 and IL-5, IL-8 in nasal polyps. Allergy 62: 66-72, 2007.
38. Yeo N, Eom D, Oh M, Lim H and Song Y: Expression of matrix metalloproteinase 2 and 9 and tissue inhibitor of metalloproteinase 1 in nonrecurrent vs recurrent nasal polyps. Ann Allergy Asthma Immunol 111: 205-210, 2013.
39. Karadag A, Fedarko N and Fisher L: Dentin matrix protein 1 enhances invasion potential of colon cancer cells by bridging matrix metalloproteinase-9 to integrins and CD44. Cancer Res 65: 11545-11552, 2005.
40. Redondo-Muñoz J, Ugarte-Berzal E, Terol M Van den Steen PE, del Cerro MH, Roderfeld M, Roeb E, Opdenakker G, García-Marco JA and García-Pardo A: Matrix metalloproteinase-9 promotes chronic lymphocytic leukemia b cell survival through its hemopexin domain. Cancer Cell 17: 160-172, 2010.

41. Ugarte-Berzal E, Bailón E, Amigo-Jiménez I, Vituri CL, del Cerro MH, Terol MJ, Albar JP, Rivas G, García-Marco JA and García-Pardo A: A 17-residue sequence from the matrix metalloproteinase-9 (MMP-9) hemopexin domain binds α4β1 integrin and inhibits MMP-9-induced functions in chronic lymphocytic leukemia B cells. J Biol Chem 287: 27601-27613, 2012.
42. Alford V, Kamath A, Ren X, Kumar K, Gan Q, Awwa M, Tong M, Seeliger MA, Cao J, Ojima I and Sampson NS: Targeting the hemopexin-like domain of latent matrix metalloproteinase-9 (proMMP-9) with a small molecule inhibitor prevents the formation of focal adhesion junctions. ACS Chem Biol 12: 2788-2803, 2017.
43. Chen S, Owens GC, Makarenkova H and Edelman DB: HDAC6 regulates mitochondrial transport in hippocampal neurons. PLoS One 5: e10848, 2010.
44. Tan HF and Tan SM: The focal adhesion protein kindlin-2 controls mitotic spindle assembly by inhibiting histone deacetylase 6 and maintaining α-tubulin acetylation. J Biol Chem 295: 5928-5943, 2020.
45. Bouvard D, Pouwels J, De Franceschi N and Ivaska J: Integrin inactivators: Balancing cellular functions in vitro and in vivo. Nat Rev Mol Cell Biol 14: 430-442, 2013.
46. Mudd PA, Katial RK, Alam R, Hohensee S, Ramakrishnan V and Kingdom TT: Variations in expression of matrix metalloproteinase-9 and tissue inhibitor of metalloproteinase-1 in nasal mucosa of aspirin-sensitive versus aspirin-tolerant patients with nasal polyposis. Ann Allergy Asthma Immunol 107: 353-359, 2011.
47. Kovacs-Kasa A, Kovacs L, Cherian-Shaw M, Patel V, Meadows M, Fulton D, Su YC and Verin AD: Inhibition of class IIa HDACs improves endothelial barrier function in endotoxin-induced acute lung injury. J Cell Physiol 236: 2893-2905, 2021.
48. Zheng Y, Chen Y, Lu X, Weng QH, Dai GL, Yu Y, Yu KH and Gao WY: Inhibition of histone deacetylase 6 by Tubastatin a attenuates the progress of osteoarthritis via improving mitochondrial function. Am J Pathol 190: 2376-2386, 2020.